

**A new method for the determination of thermal conductivity and thermal diffusivity from linear heat source measurements**

M. Banaszekiewicz, K. Seiferlin, T. Spohn, G. Kargl, and N. Kömle

Citation: [Review of Scientific Instruments](#) **68**, 4184 (1997); doi: 10.1063/1.1148365

View online: <http://dx.doi.org/10.1063/1.1148365>

View Table of Contents: <http://scitation.aip.org/content/aip/journal/rsi/68/11?ver=pdfcov>

Published by the [AIP Publishing](#)

---

**Articles you may be interested in**

[3 \$\omega\$  method for specific heat and thermal conductivity measurements](#)

Rev. Sci. Instrum. **72**, 2996 (2001); 10.1063/1.1378340

[A new thermographic methodology for 'on-site' thermal diffusivity determination](#)

AIP Conf. Proc. **463**, 392 (1999); 10.1063/1.58091

[Thermal parameters of dental materials determined by photoacoustic phase lag measurements](#)

Rev. Sci. Instrum. **69**, 3392 (1998); 10.1063/1.1149105

[Advances in the use of laser-flash techniques for thermal diffusivity measurement](#)

Rev. Sci. Instrum. **69**, 1426 (1998); 10.1063/1.1148776

[New photothermal deflection method for thermal diffusivity measurement of semiconductor wafers](#)

Rev. Sci. Instrum. **68**, 1521 (1997); 10.1063/1.1147589

---



**Not all AFMs are created equal**  
**Asylum Research Cypher™ AFMs**  
**There's no other AFM like Cypher**

[www.AsylumResearch.com/NoOtherAFMLikeIt](http://www.AsylumResearch.com/NoOtherAFMLikeIt)

**OXFORD**  
INSTRUMENTS  
*The Business of Science®*

# A new method for the determination of thermal conductivity and thermal diffusivity from linear heat source measurements

M. Banaszekiewicz

Space Research Centre, Polish Academy of Sciences, 00-716 Warsaw, Poland

K. Seiferlin and T. Spohn

Institut für Planetologie, Westfälische Wilhelms-Universität Münster, D-48149 Münster, Germany

G. Kargl<sup>a)</sup> and N. Kömle

Institut für Weltraumforschung, Österreichische Akademie der Wissenschaften, A-8010 Graz, Austria

(Received 20 December 1996; accepted for publication 5 August 1997)

The new algorithm of the thermal conductivity and thermal diffusivity determination from the transient hot-wire method has been applied to measurements performed in **several solid materials**. The algorithm makes use of the exact formula for the temperature variations, instead of its simple, asymptotic form that has been employed earlier. In the process of the least-square optimization of the residual function three parameters are obtained; thermal conductivity, thermal diffusivity, and the initial temperature. Two different variants of the method are presented: the classical one with the power kept constant during the measurements and the newly introduced constant current technique. The latter one has an advantage of requiring simpler conditioning electronics, and can therefore be recommended in space applications. The results of data processing show that thermal conductivity can be reliably determined even from the nonasymptotic part of the temperature measurements. The determination of thermal diffusivity is more difficult and requires high quality temperature data from the whole measurement interval. © 1997 American Institute of Physics.  
[S0034-6748(97)00911-8]

## I. INTRODUCTION

The transient hot-wire method has long been successfully applied to measure the thermal conductivity of gases,<sup>1</sup> liquids,<sup>2</sup> as well as solid materials.<sup>3,4</sup> In this approach, a constant power  $Q$  is continuously supplied by a current to the long, thin cylinder immersed in the medium. Heat conduction of the medium determines the rate of the temperature increase within the wire. To derive the thermal conductivity value  $\lambda$  one usually employs the asymptotic, linear part of the temperature versus  $\log$  (time) relation; its slope is inversely proportional to  $\lambda$ . It is, in principle, possible but very difficult to obtain the thermal diffusivity from measurements. It can either be done by using the initial (nonasymptotic) part of the data<sup>2</sup> or combining measurements performed for different currents,<sup>5</sup> or, with the least accuracy, by evaluation of the intersection of the tangent to the linear branch with the abscissa,  $\ln(t_0)=0$ . In the most advanced approach so far, by Håkansson *et al.*,<sup>6</sup> thermal conductivity and thermal diffusivity were both derived from the exact formula for the constant power method, valid in the whole interval of measurements. To account for power variation (the measurements were obtained for constant currents) Håkansson *et al.*<sup>6</sup> introduced corrections to the constant power expression.

Recently, thermal conductivity measurements have been proposed and accepted for several near-future planetary missions. The surface science package (SSP) experiment on the Huygens probe to Titan will contain a couple of thermal conductivity sensors to measure the properties of the planet's atmosphere as well as of the hypothetical ocean on the surface.<sup>7</sup> The penetrator-temperature profile penetrator-

thermal conductivity (PEN-TP+PEN-THC) probe, a part of the multipurpose sensors for surface and subsurface science (MUPUS) experiment suite, is going to be sent to comet Wirtanen on board the RoLand lander during the Rosetta mission in order to determine the thermal conductivity of the subsurface layer.<sup>8</sup> Space experiments put very stringent constraints on the experimental setup and available resources (mass, power, data rate, etc.), therefore it is natural in this context to extract as much as possible from the available data and to design the experiment in the optimal way. For example, a lot can be gained if the constant power method is replaced by the technically much simpler constant current method. Similarly, a lot of power will be spared on the average if the thermal conductivity is determined from a short duration measurement, even though the asymptotic limit is not reached.

In this study we want to address three of such issues. First, we present the full, nonasymptotic formulae for both the constant power and the constant current method. The former has long since been used (theory and references to the earlier papers are given in Ref. 9), but, to our knowledge, the latter has never been described. Second, we show how to obtain the thermal conductivity from an arbitrary subinterval of the whole data set proving in this way that it is not necessary to use exclusively the temperature data from the asymptotic range. Finally, we demonstrate that it is possible to derive also the thermal diffusivity from measurements, although less accurately than the thermal conductivity. Concerning the second and the third issue, we come to a similar qualitative evaluation of the method as given by Håkansson *et al.*,<sup>6</sup> although we have used a completely different experimental setup and applied a new method of data processing. Since, in many cases, it is difficult to directly compare thermal parameters obtained from measurements with the values

<sup>a)</sup>Also at Max-Planck-Institut für Aeronomic, D-37191 Katlenburg-Lindau, Germany.

referenced in the literature because of a different type of material used or a different method of sample preparation, we will focus our attention on the performance of the algorithm and the internal consistency of results. We start with the short presentation of equations, followed by a brief description of the experiments and by the presentation of results obtained for different compact and granular materials: teflon, dunite powder, compact, and porous water ice. Part of the experimental data and the interpretation in terms of the asymptotic formula for the thermal conductivity has already been published by Seiferlin *et al.*<sup>4</sup> In the last section we discuss the application of the method to the space experiments and summarize our work.

## II. METHOD OF DATA INTERPRETATION

We use the standard experimental configuration for the hot-wire method and, following other researchers,<sup>1,2,9,10</sup> model it as an infinite cylindrical source of heat power surrounded by a uniform medium characterized by density  $\rho$ , thermal conductivity  $\lambda$ , and specific heat  $c$ . The wire with a radius  $r$ , density  $\rho_w$ , and specific heat  $c_w$ , is assumed to be a perfect heat conductor with the thermal capacity per unit length  $S = 2\pi r^2 \rho_w c_w$ . We neglect the heat resistance between the wire and the medium. If the power dissipated per unit length is  $q$ , then the temperature of the wire  $T$  will vary with time  $t$  according to the formula

$$T - T_0 = \frac{2q\alpha^2}{\pi^3\lambda} \int_0^\infty \frac{1 - \exp(-atu^2/r^2)}{u^3\Delta(u, \alpha)} du, \quad (1)$$

where  $T_0$  is the initial temperature at the moment of the power switch on,  $a = \lambda/\rho c$  is the thermal diffusivity, and  $\alpha = 2\rho c/\rho_w c_w$ . The denominator in (1) depends on the Bessel functions  $J_0$ ,  $J_1$ ,  $Y_0$ , and  $Y_1$ :

$$\Delta(u, \alpha) = [uJ_0(u) - \alpha J_1(u)]^2 + [uY_0(u) - \alpha Y_1(u)]^2. \quad (2)$$

In the case of the constant current  $I$ , the power changes linearly with the temperature due to an increasing resistance  $R$  of the wire:

$$\begin{aligned} q(t) &= I^2 R(t) = I^2 R_0 \{1 + \beta [T(t) - T_0]\} \\ &= q_0 + q_1 (T - T_0). \end{aligned} \quad (3)$$

It can be shown that the temperature variations in this case are described by an expression similar to (1), but with  $q_0$  instead of  $q$  in the factor multiplying the integral, and with  $\Delta$  replaced by  $\Delta_h$ :

$$\begin{aligned} \Delta_h(u, \alpha) &= \left[ u \left( 1 + \frac{q_1 r^2}{S a u^2} \right) J_0(u) - \alpha J_1(u) \right]^2 \\ &+ \left[ u \left( 1 + \frac{q_1 r^2}{S a u^2} \right) Y_0(u) - \alpha Y_1(u) \right]^2. \end{aligned} \quad (4)$$

The asymptotic expansion of (1), valid for large  $t$  ( $at/r^2 \gg 1$ ), reads

$$T - T_0 = \frac{q}{4\pi\lambda} [-0.5772 + \ln(4at/r^2)], \quad (5)$$

and allows us to directly determine  $\lambda$  from the slope of  $T(\ln t)$ . This approach is commonly used to evaluate experimental data (e.g., Refs. 1 and 4). In general, however, and especially for  $t \ll a/r^2$ , the exact formula (1) with (2) or (4) should be used.

There are three unknown parameters in (1);  $\lambda$ ,  $\rho c$ , and  $T_0$ . We introduce a new set of unknowns;

$$x_1 = \frac{\lambda}{\lambda_{\text{ref}}}, \quad x_2 = \frac{\alpha}{\alpha_{\text{ref}}}, \quad x_3 = T_0, \quad (6)$$

by normalizing  $\lambda$  and  $\alpha$  to their reference values  $\lambda_{\text{ref}}$  and  $\alpha_{\text{ref}}$ .

The expected results of an ideal temperature measurement at  $t_i$  are then equal to:

$$\begin{aligned} T_i^c &= T^c(t_i; x_1, x_2, x_3) \\ &= x_3 + \frac{2q\alpha_{\text{ref}}^2 x_2^2}{\pi^3 \lambda_{\text{ref}} x_1} \\ &\quad \times \int_0^\infty \frac{1 - \exp(-2\lambda_{\text{ref}} \rho_w c_w t u^2 x_1 / r^2 \alpha_{\text{ref}} x_2)}{u^3 \Delta(u, x_1, x_2)} du. \end{aligned} \quad (7)$$

A time sequence of real measurements  $T_i^o$ ,  $i = 1, \dots, N$  can now be compared with corresponding  $T_i^c$  in order to find the values of  $x_1, x_2, x_3$  that give the minimum of the sum of squared residuals:

$$L = L(x_1, x_2, x_3) = \sum_{i=1}^N [T_i^o - T_i^c(x_1, x_2, x_3)]^2. \quad (8)$$

Since  $T_i^c$  is a nonlinear function of  $x_1, x_2$  we will find the minimum of  $L$  by applying an optimization method. Once the optimal  $x_1, x_2, x_3$  are known, it is straightforward to obtain  $\lambda$ ,  $a$ , and  $T_0$  from (6). Our method of data evaluation differs in many respects from that employed by Håkansson

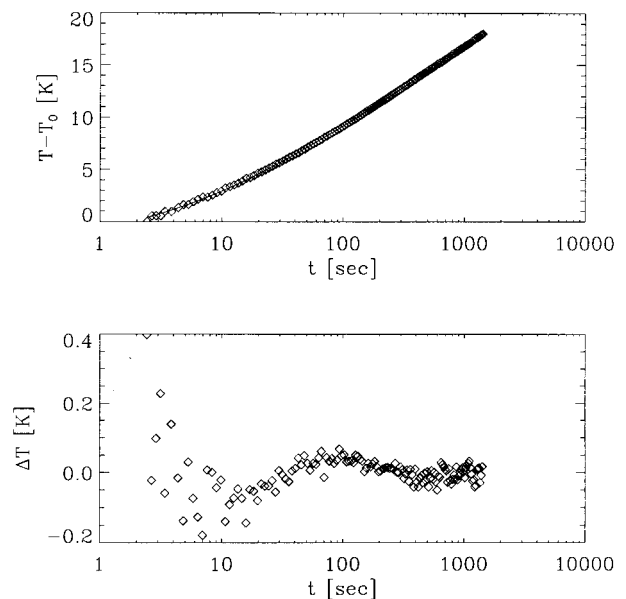


FIG. 1. Upper panel: The data (diamonds) and the optimal fit (solid line) obtained for the teflon data set T18 (constant current). Lower panel: The difference (residuum) between the temperature calculated according to (1) and observed temperature for the same data set.

TABLE I. Teflon.

Data set <sup>a</sup>	No. of points	Subinterval (points)	$\lambda$ (W/mK)	$a$ (m <sup>2</sup> /s)	$T_0$ (C)	Average residuum (K)	$\lambda_{asm}$ <sup>b</sup> (W/mK)
T18	144	1–144	0.242	1.36E-7	21.64	0.057	0.242–0.237
T10	144	1–144	0.245	1.68E-7	22.65	0.082	0.258–0.243
T20	144	1–144	0.248	1.77E-7	22.71	0.062	0.249–0.243
T21	144	1–144	0.247	1.74E-7	23.28	0.053	0.255–0.240
T22	160	1–160	0.247	1.75E-7	22.77	0.052	0.245–0.239
T23	160	1–160	0.249	1.97E-7	20.78	0.060	0.248–0.240
T24	160	1–160	0.248	1.94E-7	21.49	0.058	0.248–0.240
T25	144	1–144	0.243	1.80E-7	22.09	0.074	0.243–0.237
T26	144	1–144	0.262	2.38E-7	31.01	0.089	0.282–0.252
T28	144	1–144	0.251	1.56E-7	21.88	0.046	0.256–0.251
T29	144	1–144	0.251	2.32E-7	21.94	0.058	0.258–0.249
T30	144	1–144	0.252	1.85E-7	21.83	0.044	0.247–0.243
T31	144	1–144	0.249	2.15E-7	21.93	0.065	
T18	30	21–50	0.228	0.86E-7	22.25	0.021	
T19	30	21–50	0.258	1.82E-7	22.90	0.032	
T20	30	21–50	0.236	1.14E-7	23.35	0.026	
T21	30	21–50	0.255	1.70E-7	23.52	0.026	
T22	30	21–50	0.262	2.02E-7	22.91	0.024	
T23	30	21–50	0.242	1.37E-7	21.36	0.021	
T24	30	21–50	0.243	1.48E-7	21.91	0.026	
T28	30	21–50	0.244	1.12E-7	22.26	0.020	
T29	30	21–50	0.223	0.98E-7	22.86	0.024	
T30	30	21–50	0.215	0.69E-7	22.51	0.017	
T31	30	21–50	0.265	2.45E-7	22.13	0.025	
T18	72	37–108	0.237	1.18E-7	21.80	0.016	
T19	72	37–108	0.237	1.28E-7	23.09	0.026	
T20	72	37–108	0.244	1.59E-7	22.79	0.025	
T21	72	37–108	0.241	1.43E-7	23.48	0.016	
T22	80	41–108	0.247	1.91E-7	22.47	0.022	
T23	80	41–108	0.247	2.27E-7	20.27	0.021	
T24	80	41–108	0.241	1.49E-7	21.84	0.016	
T28	72	37–108	0.255	2.27E-7	21.18	0.027	
T29	72	37–108	0.250	2.48E-7	21.67	0.017	
T30	72	37–108	0.253	2.46E-7	21.33	0.024	
T31	72	37–108	0.246	1.96E-7	21.98	0.022	

<sup>a</sup>Data sets T24 and T25 correspond to the constant power mode, the remaining ones to the constant current mode.

<sup>b</sup> $\lambda_{asm}$  is obtained from formula (5) using the running-box five-point linear approximation of measurements.

*et al.*<sup>6</sup> First of all, we use a specialized optimization routine E04LBF from the Numerical Algorithms Group (NAG) library. At each step of optimization, expression (7), as well as its first and second partial derivatives with respect to  $x_1$  and  $x_2$ , are calculated explicitly by an adaptive Gaussian quadrature with an accuracy of  $10^{-8}$ . The average CPU time of processing one data set is about 1 min on a PC-486.

### III. RESULTS

The measurements have been performed for different materials (compact and granular) in various experimental conditions (pressure, temperature). The details of experimental setup and data acquisition have been explained by Seifertlin *et al.*<sup>4</sup> In short, the thermal probe comprises a thin (radius 1 mm) hollow aluminum cylinder with a copper wire (radius 0.03 mm) tightly coiled around it. The wire serves, at the same time, as a heat source and a resistance-type temperature sensor.

We describe first the results for teflon, which can be considered as a reference material with well known and

stable values of thermal conductivity and thermal diffusivity.<sup>11</sup> Next, we present the measurements and their interpretation for a granular material, dunite. Finally, we show the results for compact and porous ice. The experiments with dunite and the ices have been carried out in the constant power mode. The exact formula for the constant current method has been derived later and checked on the teflon data.

The issues of particular interest are; (i) the thermal parameter determination from the exact formula (1) as compared with the asymptotic expression (5), (ii) the dependence of the parameter values on the data subinterval used, and (iii) the comparison of the constant power and the constant current methods.

#### A. Teflon

The measurements have been made in normal conditions, i.e., at room temperature and atmospheric pressure. The sensor has been immersed into a hole drilled in a teflon block. To ensure a good thermal contact between the sensor

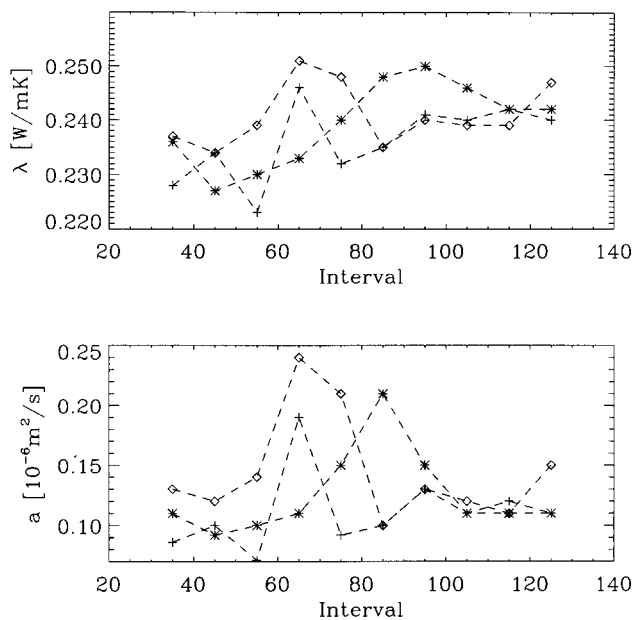


FIG. 2. Thermal conductivity (upper panel) and thermal diffusivity (lower panel) of teflon as determined from 30 data points centered at the point number given by the abscissa. The curves correspond to the following data sets: T18 (+), T20 (\*), and T24 (◇).

and the medium, the free space (approximately 0.5–1 mm gap) in the hole has been filled with pump oil, which can be considered as a perfect conductor (due to the convection effect, see Ref. 9). Both the constant power and the constant

current methods have been tested. A typical run for a constant current of 175 mA is presented in Fig. 1. The solid line in the upper panel corresponds to the best fit values of thermal parameters. The scatter of residuals (i.e.,  $T_i^c - T_i^0$ ) that are presented in the lower panel indicate that the systematic (model) errors are rather small. The larger residuals in the initial part of the data are due to a limited resolution of the analog-to-digital (ADI) converter. The amplitude of residuals is larger for the constant power than for the constant current, which follows from inaccuracy in stabilizing the power. The thermal conductivity and diffusivity obtained from processing the data from several measurements are presented in Table I. In the second part of this table the values obtained from different subintervals of the whole data sets are shown. The nominal values given by Grigull and Sandner<sup>11</sup> are  $\lambda = 0.23$  and  $a = 1 \times 10^{-7}$ ; Goodfellow, a company which sells all sorts of materials and specimens, gives  $\lambda = 0.25$  in their 1995/1996 catalogue. It is evident that the accuracy of the thermal conductivity determination is quite good even for the early part of the data set ( $t \leq t_{asm} = r^2/a$ ). Thermal diffusivity, on the other hand, shows much larger scatter for smaller subintervals as compared with the values derived from all data points. Applying the standard estimators of the expected value and its variance to the constant current results and the whole data sets, we obtain  $\lambda = 0.246$  W/m K,  $\Delta\lambda = 0.0035$  W/m K,  $a = 0.183 \times 10^{-6}$  m<sup>2</sup>/s, and  $\Delta a = 0.025 \times 10^{-6}$  m<sup>2</sup>/s. The values for a 30-point subinterval (points 21 to 50 of each data set) corresponding to  $9 < t < 50$  s are  $\lambda = 0.243$  W/m K,  $\Delta\lambda = 0.015$  W/m K,  $a = 0.142$

TABLE II. Dunite.

Data set <sup>a</sup>	No. of points	Subinterval (points)	$\lambda$ (W/mK)	$a$ (m <sup>2</sup> /s)	$T_0$ (C)	Average residuum (K)	$\lambda_{asm}^b$ (W/mK)
DU11	50	1–50	0.283	7.08E-7	29.26	0.141	0.278–0.258
DU14	50	1–50	0.0547	1.29E-7	48.71	0.346	0.058–0.049
DU15	50	1–50	0.0547	0.74E-7	27.17	0.183	0.056
DU18	49	2–50	0.0376	0.49E-7	40.94	0.231	0.037
DU19	50	1–50	0.0350	0.42E-7	44.08	0.282	0.037
DU20	50	1–50	0.0336	0.43E-7	43.09	0.317	0.036
DU21	50	1–50	0.0345	0.39E-7	39.02	0.212	0.038
DU22	50	1–50	0.0502	0.74E-7	42.44	0.198	0.053–0.051
DU11	15	11–25	0.312	9.53E-7	29.32	0.101	
DU14	15	11–25	0.0392	0.41E-7	48.90	0.130	
DU15	15	11–25	0.0560	0.94E-7	26.62	0.105	
DU18	15	11–25	0.0458	1.18E-7	40.08	0.140	
DU19	15	11–25	0.0328	0.34E-7	43.93	0.137	
DU20	15	11–25	0.0217	0.12E-7	43.22	0.112	
DU21	15	11–25	0.0251	0.16E-7	39.07	0.149	
DU22	15	11–25	0.0564	2.01E-7	41.90	0.197	
DU11	27	11–37	0.245	2.30E-7	29.62	0.113	
DU14	27	11–37	0.0525	1.31E-7	48.06	0.165	
DU15	27	11–37	0.0589	1.14E-7	26.51	0.110	
DU18	27	11–37	0.0388	0.63E-7	40.35	0.163	
DU19	27	11–37	0.0279	0.21E-7	44.05	0.139	
DU20	27	11–37	0.0277	0.25E-7	42.94	0.118	
DU21	27	11–37	0.0320	0.32E-7	38.85	0.140	
DU22	27	11–37	0.0490	0.74E-7	42.25	0.190	

<sup>a</sup>All data sets measured in the constant power mode, at different pressures: GDU11–10<sup>5</sup> Pa, GDU14–1×10<sup>-2</sup>–7×10<sup>-2</sup> Pa, GDU15–4×10<sup>-1</sup> Pa, GDU18–4.2×10<sup>-3</sup> Pa, GDU19–4×10<sup>-3</sup> Pa, GDU20–1×10<sup>-2</sup> Pa, GDU21–5×10<sup>-2</sup> Pa, and GDU22–1×10<sup>-1</sup> Pa.

<sup>b</sup> $\lambda_{asm}$  is obtained from formula (5) using the running-box five-point linear approximation of measurements.

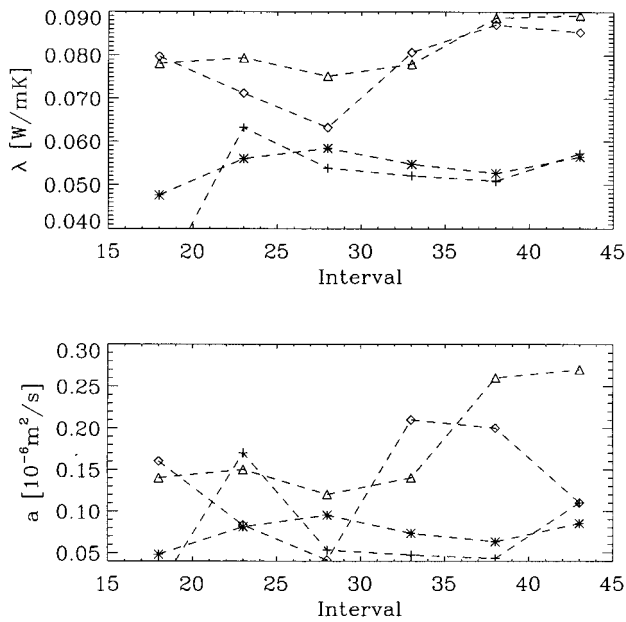


FIG. 3. The same as Fig. 2, but for the dunite data sets: DU15 with  $T_0$  determined independently for each subinterval (+), DU15 with the same  $T_0$  for all subintervals (\*), DU24 with  $T_0$  determined independently ( $\diamond$ ), and DU24 with the same  $T_0$  ( $\triangle$ ). Note that DU15 and DU24 have been obtained at different pressures and, therefore, should give different values for the thermal conductivity.

$\times 10^{-6} \text{ m}^2/\text{s}$ , and  $\Delta a = 0.051 \times 10^{-6} \text{ m}^2/\text{s}$ . Finally, taking the subinterval in the middle of the set that consists of about half of the total points in the whole interval, one gets  $\lambda = 0.245 \text{ W/m K}$ ,  $\Delta\lambda = 0.0057 \text{ W/m K}$ ,  $a = 0.185 \times 10^{-6} \text{ m}^2/\text{s}$ , and  $\Delta a = 0.045 \times 10^{-6} \text{ m}^2/\text{s}$ . For the measurements in the whole interval, the obtained values of the thermal conductivity and thermal diffusivity are larger by more than one standard deviation from their nominal values given by Grigull and Sandner.<sup>11</sup> This effect may be explained by the systematic error caused by the conducting layer (oil) placed between the sensor and the medium [which is not taken into account in formulae (1) or (3)]. Therefore, in the following we will concentrate on the consistency of data rather than on their close agreement with the reference values.

It is interesting that if one shifts a 30-point subinterval, from which the data are processed, through the whole data

set, then the thermal parameters determined at the beginning and at the end of the whole set are quite similar. There are, however, differences for the middle part (Fig. 2). We explain this effect by some small systematic effects not taken into account in the model: the thermal resistance between the probe and the medium, for example. It is somehow amplified and apparently shows only in a certain part of the measurements.

The asymptotic formula (5) was used to approximate sets of five consecutive measurement points by straight lines and derive  $\lambda$  (the running-box five-point linear approximation). The values obtained in that way are similar, though slightly larger than those found in the nonlinear fit.

Finally, we checked how the inaccuracies in parameters that enter formula (1) but are not optimized, such as  $\rho_w c_w$  and  $r$ , could affect the results. It appeared that even for a 30% change in any of them the thermal conductivity does not vary by more than 1%. The thermal diffusivity value is insensitive to changes in  $\rho_w c_w$  but vary approximately as  $1/r^2$  with the radius of the heating rod.

## B. Dunite

The thermal conductivity of this mineral powder has been measured in a vacuum recipient at room temperature at different pressures, ranging from  $10^{-3}$  to  $10^5 \text{ Pa}$  (Ref. 4). All measurements have been done in the constant power mode. Table II contains the parameters determined in different subintervals for several data sets. There is an obvious difference with respect to the teflon measurements; the dunite parameters strongly depend on the subinterval. The values obtained from the last subinterval (points 38–50) are, in general, consistent with the values derived from the whole set. Also, the parameters found from the fit in the middle subinterval (points 12–38) are reasonably close to those obtained from fitting to all points. The effect can be, in part, explained by (i) employing the less accurate constant power method, and (ii) using the smaller number of points in the fitting process than for teflon. Even though the parameters obtained from small subintervals are, on the average, determined with large errors (which is indicated by a large scatter of their values), there are data sets (Fig. 3) which give consistent results for all subintervals.

From the thermal conductivity and thermal diffusivity

TABLE III. Compact ice.

Data set <sup>a</sup>	No. of points	Subinterval (points)	$\lambda$ (W/mK)	$a$ ( $\text{m}^2/\text{s}$ )	$T_0$ (C)	Average residuum (K)	$\lambda_{\text{asm}}^b$ (W/mK)
CI02	50	1–50	5.92	3.23E-5	–199.93	0.110	8.1–5.7
CI03	50	1–50	5.24	2.86E-5	–200.10	0.095	7.5–5.0
CI04	50	1–50	5.66	3.08E-5	–199.88	0.098	8.5–4.0
CI08	49	2–50	1.96	2.23E-6	–67.63	0.084	2.1
CI09	50	1–50	2.08	1.07E-5	–67.08	0.071	2.15
CI10	50	1–50	2.20	1.20E-5	–66.62	0.088	2.15
CI29	50	1–50	2.15	1.17E-5	–25.78	0.128	2.5
CI30	50	1–50	2.31	1.26E-5	–24.66	0.202	
CI31	50	1–50	2.29	1.25E-5	–24.83	0.192	2.3

<sup>a</sup>All data sets measured in the constant power mode.

<sup>b</sup> $\lambda_{\text{asm}}$  is obtained from formula (5) using the running-box five-point linear approximation of measurements.

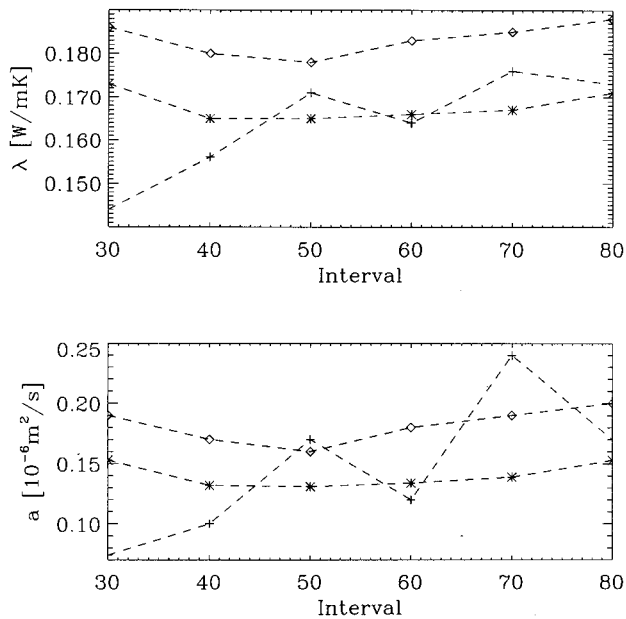


FIG. 4. The same as Fig. 2, but for the compact ice data sets: CI31 (+), CI02 (\*), and CI10 (◇). In all cases  $T_0$  was determined independently in each subinterval.

one can determine the product  $\rho c$  which should not depend on the pressure. This parameter, when determined from the whole intervals of 12 data sets, is in the range  $5.5\text{--}8.5 \times 10^5 \text{ J/m}^3 \text{ K}$ .

### C. Compact ice

The sensor was slowly frozen into the ice: it was fixed in its final position within the sample container, which was cooled by liquid nitrogen. Shallow layers of water have been poured into the sample container, freezing and thus forming a solid ice block with layering in the  $z$  direction. Thermal cracks, which formed close to the sensor, and small pores did not ensure a good contact between the ice and the sensor. Therefore, one might expect a substantial thermal resistance which could modify the value of thermal conductivity. The ice temperature was varied from 73 to 250 K. The pressure was atmospheric. The difference between the temperature profiles for the compact ice on one side and granular materials on the other (Fig. 1) is that the ice curve is approximately a straight line with only a trace of curvature. This shape of the temperature function results from a high thermal conductivity of ice, which is an order of magnitude larger than that for the granulates (e.g., dunite). As a consequence, the temperature profile of ice reaches the asymptotic region in much shorter time. Since the thermal diffusivity can be at best determined from the initial, nonasymptotic part of the profile, which in the case of compact ice is almost absent, one can expect that the determination of  $a$  will be difficult. Indeed, the scatter of diffusivity values obtained from different data sets or different subintervals within one set shows that the reliable value of  $a$  can only be obtained for particular data sets, for which the systematic errors are small and the temperature is measured with high accuracy (Table III, Fig. 4). The thermal conductivity should follow the dependence

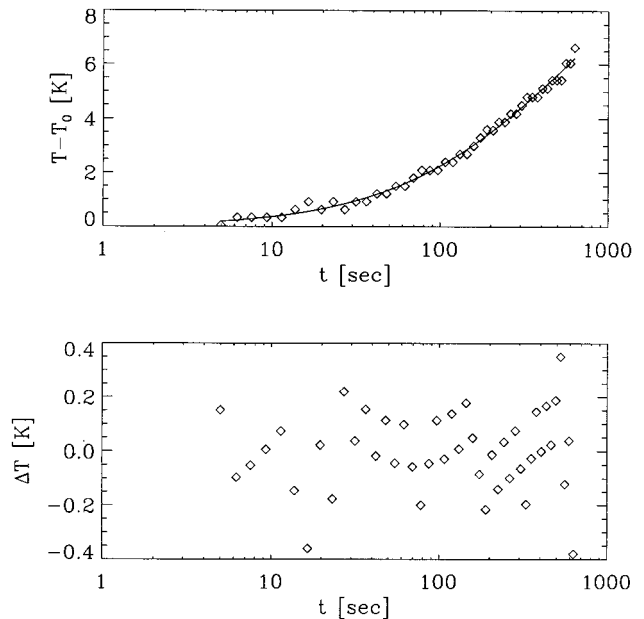


FIG. 5. The same as Fig. 1, but for the porous ice data set PI03 (constant power).

$567/T[\text{K}]\text{W/m K}$  (Ref. 12). The values obtained by us are smaller by about 20%, which can be explained by the instrumental effects mentioned earlier (cracks in the sample, poor thermal contact).

In all runs of the optimization code the obtained values of  $a$  and  $T_0$  were strongly correlated, but almost independent of  $\lambda$ . In such a case, one can approach the problem of thermal diffusivity determination from another side: first to determine a  $T_0$  value from the initial part of the temperature profile and then to process the following subintervals, optimizing (5) with respect to only two parameters  $\lambda$  and  $a$ . This method gives much more consistent values of  $a$  (Table III).

### D. Porous ice

Since porous ice is characterized by a high sticking coefficient, the thermal contact between the sensor and the sample is similar to the thermal contact within the ice (5%), contrary to the case of compact ice, where the contact area is almost 100% within the ice but is reduced to about 80% at the sensor–medium interface. Thermal conductivity of porous materials is low and the measured temperature profile does not reach the asymptotic range even for  $t = 1000 \text{ s}$  (Fig. 5). For the thermal conductivity we get  $\lambda = 0.00416 \text{ W/m K}$ , which, at  $T = 137 \text{ K}$  and at the low pressure applied ( $< 10^{-3} \text{ Pa}$ ), corresponds to the Hertz factor  $\beta = 0.001$ . The determined value of  $a$  should be about  $7.5 \times 10^{-8} \text{ m}^2/\text{s}$ , if we substitute  $\rho c$  of ice with a porosity 0.5.<sup>11</sup> In fact, we have obtained  $a = 7.8 \times 10^{-8} \text{ m}^2/\text{s}$ , which is a rather fortunate agreement taking into account large errors of single measurements (Fig. 5, lower panel). Interestingly enough, this diffusivity value can only be obtained from optimization in the whole interval, or, in the second half of it. Any attempt to reproduce this value from processing the initial part of the data fails.

#### IV. DISCUSSION

We have applied a new algorithm of thermal conductivity and thermal diffusivity determination from the hot-wire transient temperature measurements in solids. The method evaluates the data from the arbitrary measurement interval, contrary to the commonly used approach, in which only the data from the asymptotic interval ( $t > t_{\text{asm}}$ ) are processed in order to derive the thermal conductivity value. An interesting extension of the constant power formula for the temperature variations allows us to interpret the data obtained in the constant current mode.

In general, the thermal conductivity determination from the whole data interval gives a very similar value to that obtained from the asymptotic formula, but has an advantage of employing more data points which results in a better accuracy (smaller errors) of  $\lambda$ . It is also possible to derive a reliable value of thermal conductivity from the initial, non-asymptotic part of the measurements. Theoretically, the quality of the fit, for the comparable number of points, should be the same as from the asymptotic part of the data. In the case of our measurements, however, it is difficult to directly compare the accuracy of both  $\lambda$  determinations because of (i) a better resolution of temperature data in the asymptotic interval, and (ii) small systematic errors in data due to neglecting the thermal resistance between the probe and the medium.

The new method gives a possibility of obtaining another parameter of the medium from the data fit: the thermal diffusivity. Since the optimized function is much less sensitive to the thermal diffusivity than to the thermal conductivity the determination of the former parameter is, however, difficult, and requires a high accuracy of temperature measurements. Indeed, when the thermal diffusivity is determined from the constant current runs, which due to technical reasons are definitely better than the constant power data, the values of  $a$  are more consistent. In the best cases the estimated error of  $a$  is about 15%, while the corresponding error for the thermal conductivity amounts to a few percent. The errors can be made smaller if the accuracy of a single temperature measurement is increased. A 0.01 K accuracy of temperature data should guarantee the thermal diffusivity determination with an error of about 5%.

The presented method has a number of advantages in space applications. First, when the constant current mode is used, the instrument electronics can be simpler and the stability of the input parameter (current) is better controlled. Second, the duration of the measurement interval can be significantly reduced without the loss of accuracy of the determined parameters. Such shortening will result in smaller average power consumption (first 50% of the total data points

correspond to 10%–15% of the total duration and energy needed) or/and a possibility of more frequent repetition of the measurement cycle. Third, the method can give an estimate of the thermal diffusivity without introducing any independent measurements.

The development of the described technique can proceed in two directions. On the technical side, it would be desirable to measure the temperature more accurately in a shorter time interval. Fortunately, this does not put any additional requirement on the resolution of the analog–digital converter used. As for the algorithm of the data processing, it should be generalized to include the case of a poor thermal contact between the sensor and the surrounding environment, thermal properties of which are going to be measured. Such an improvement is possible, but it will introduce a new optimization parameter—the thermal resistance.<sup>9</sup> On one hand the algorithm will become more complicated, on the other it will allow us to get new information about the medium; thermal resistance can be interpreted in terms of its porosity, Hertz factor, number of cracks per unit volume, etc., provided that the contact area between the sensor and the medium is typical for the medium itself. At last, one can try to apply a recently developed multicurrent method, in which the hot-wire measurements are repeated with different current intensities, in order to simultaneously determine the thermal conductivity and thermal diffusivity from the asymptotic formula (3).

#### ACKNOWLEDGMENTS

The work was supported in part by the Polish Committee for Scientific Research Grant No. 2 Z600 006 06 (M.B.), the Austrian ‘‘Fonds zur Förderung der wissenschaftlichen Forschung’’ under project P8689-TEC, and by DARA (K.S.).

- <sup>1</sup>J. J. De Groot, J. Kestin, and H. Sookozian, *Physica A* **78**, 454 (1974).
- <sup>2</sup>O. Sandberg, P. Andersson, and G. Bäckström, *J. Phys. E* **10**, 474 (1977).
- <sup>3</sup>K. Buettner, *Trans. AGU* **36**, 831 (1955).
- <sup>4</sup>K. Seiferlin, N. I. Kömle, G. Kargl, and T. Spohn, *Planet. Space Sci.* **44**, 691 (1996).
- <sup>5</sup>H. Takahashi, Y. Hiki, and Y. Kogure, *Rev. Sci. Instrum.* **65**, 2901 (1994).
- <sup>6</sup>B. Håkansson, P. Andersson, and G. Bäckström, *Rev. Sci. Instrum.* **59**, 2269 (1988).
- <sup>7</sup>P. N. W. Birchley, P. M. Daniell, J. C. Zarnecki, and D. J. Parker, *Proceedings of the Symposium on Titan, 1992* (unpublished), p. 311, ESA SP-338.
- <sup>8</sup>T. Spohn *et al.* (unpublished).
- <sup>9</sup>H. S. Carslaw and J. C. Jaeger, *Conduction of Heat in Solids*, 2nd edition (Oxford University Press, Oxford, 1959).
- <sup>10</sup>E. McLaughlin and J. F. T. Pittman, *Philos. Trans. R. Soc. London, Ser. A* **270**, 557 (1971).
- <sup>11</sup>U. Grigull and H. Sandner, *Heat Conduction* (Springer-Verlag, Berlin, 1984).
- <sup>12</sup>J. Klinger, *Icarus* **47**, 320 (1981).